PROCEEDINGS OF SCIENCE

Exclusive vector meson production in electron - ion collisions at the future colliders

Celso R. Sena,[a,*] **Victor P. Gonçalves**[a] **and Daniel E. Martins**[a]

[a] *High and Medium Energy Group, Instituto de Física e Matemática, Universidade Federal de Pelotas (UFPel),*
Caixa Postal 354, 96010-900, Pelotas, RS, Brazil
E-mail: celsorodriguessena@gmail.com, barros@ufpel.edu.br, dan.ernani@gmail.com

The exclusive vector meson production in electron - ion collisions for the energies of the future colliders is investigated considering the possible states of nucleon configurations in the nuclear wave function and taking into account of the non-linear corrections to the QCD dynamics. The results for the coherent and incoherent ϕ and J/ψ production in eAu collisions indicate that a future experimental analysis of these processes can be useful to constrain the description of the QCD dynamics at high energies.

XV International Workshop on Hadron Physics (XV Hadron Physics) 13 -17 September 2021
Online, hosted by Instituto Tecnológico de Aeronáutica, São José dos Campos, Brazil

PoS(XVHadronPhysics)041

---

[*] Speaker

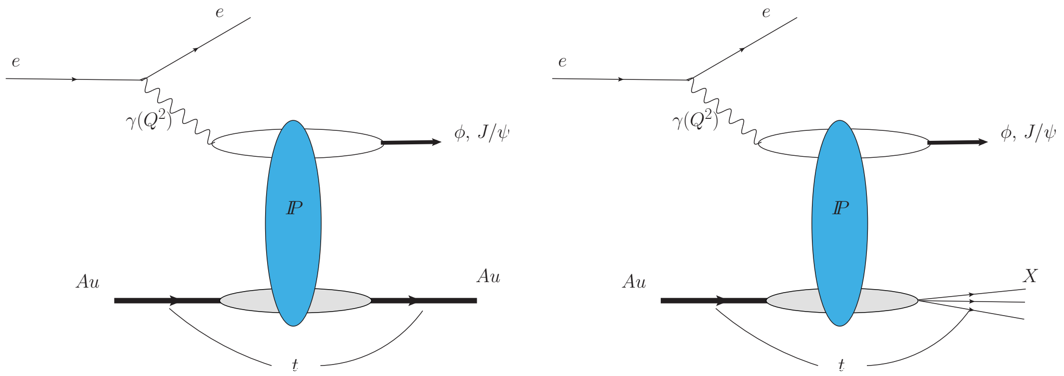

(a) (b)

Figure 1: Typical diagrams for the (a) coherent and (b) incoherent vector meson production in electron – ion collisions.

1. Introduction

Electron-nucleus colliders are the ideal facilities to improve our understanding of the strong interactions theory - the Quantum Chromodynamics (QCD) - in the high energy regime, where the gluons play a dominant role in the hadron structure and non-linear (saturation) effects are expected to become important [1]. In particular, electron - nucleus collisions are considered ideal to probe the saturation regime [2]. One of the most promising observables to probe the gluonic structure of nuclei and the high - density regime of QCD is the exclusive vector meson production off large nuclei in coherent and incoherent interactions, represented in Figs. 1 (a) and (b), respectively. Both processes are characterized by the presence of a rapidity gap in the final state, due to the color singlet exchange. However, if the nucleus scatters elastically, the process is called coherent production. On the other hand, if the nucleus scatters inelastically, the process is denoted incoherent production and one sums over all final states of the target nucleus, except those that contain particle production. In Ref. [3] we have estimated the coherent and incoherent ϕ and J/ψ production in eAu collisions considering the possible states of nucleon configurations in the nuclear wave function and taking into account of the non-linear corrections to the QCD dynamics. In what follows we will present a brief summary of the results derived in Ref. [3].

2. Formalism

In the color dipole formalism, the scattering amplitude can be factorized in terms of the fluctuation of the virtual photon into a $q\bar{q}$ color dipole, the dipole-nucleus scattering by a color singlet exchange ($\mathbb{P}$) and the recombination into the exclusive final state, being given by (See, e.g. Ref. [4]).

$$\mathcal{A}_{T,L}(x,Q^2,\Delta) = i\int d^2\mathbf{r}\int\frac{dz}{4\pi}\int d^2\mathbf{b}\, e^{-i[\mathbf{b}-(1-z)\mathbf{r}].\mathbf{d}}\ (\Psi^{V*}\Psi)_{T,L}\ \frac{d\sigma_{dA}}{d^2\mathbf{b}}(x,\mathbf{r},\mathbf{b}) \qquad (1)$$

where $\Delta = \sqrt{-t}$ is the momentum transfer, Q^2 is the photon virtuality and $x = (M^2+Q^2-t)/(W^2+Q^2)$, with W being the center of mass energy of the virtual photon - nucleus system and M the mass of the vector meson. The variables $\mathbf{r}$ and z are the dipole transverse radius and the momentum fraction of the photon carried by a quark (an antiquark carries then $1 - z$), respectively, and $\mathbf{b}$ is the impact parameter of the dipole relative to the target. Moreover, $(\Psi^{V*}\Psi)_i$ is the wave function overlap between the virtual photon and the vector meson wave functions, will be described using the Boosted Gaussian model (For details see e.g. Ref. [5]) and $d\sigma_{dA}/d^2\mathbf{b}$ is the dipole-nucleus cross section (for a dipole at impact parameter $\mathbf{b}$) which encodes all the information about the hadronic scattering, and thus about the non-linear and quantum effects in the hadron wave function [1]. The differential cross sections for the coherent and incoherent interactions are given by

$$\left.\frac{d\sigma^{\gamma^* A \to V A}}{dt}\right|_{T,L}^{coh} = \frac{1}{16\pi} \left|\left\langle \mathcal{A}_{T,L}(x, Q^2, \Delta)\right\rangle\right|^2 , \tag{2}$$

and

$$\left.\frac{d\sigma^{\gamma^* A \to V X}}{dt}\right|_{T,L}^{inc} = \frac{1}{16\pi} \left(\left\langle\left|\mathcal{A}_{T,L}(x, Q^2, \Delta)\right|^2\right\rangle - \left|\left\langle \mathcal{A}_{T,L}(x, Q^2, \Delta)\right\rangle\right|^2\right), \tag{3}$$

where $\langle ... \rangle$ represents the average over the configurations of the nuclear wave function and $X = A^*$ is the dissociative state generated in the incoherent interaction.

In our analysis we will consider two distinct models for QCD dynamics for the J/ψ and ϕ production in the kinematics relevant for the EIC, LHeC and FCC-eh. We will present predictions for the transverse momentum distributions, obtained taking into account of the saturation effects, and the results will be compared with those derived disregarding these effects. In particular, for the saturated case, we will describe the dipole - nucleus cross section using the Glauber-Gribov formalism [6], which implies that $d\sigma_{dA}/d^2\mathbf{b}$ is given by

$$\frac{d\sigma_{dA}}{d^2\mathbf{b}} = 2\left(1 - \exp\left[-\frac{1}{2}\,\sigma_{dp}(x, \mathbf{r}^2)\,T_A(\mathbf{b})\right]\right) , \tag{4}$$

where σ_{dp} is the dipole-proton cross section and $T_A(\mathbf{b})$ is the nuclear profile function. For comparison, we also will present predictions derived disregarding the saturation effects, with the dipole-nucleus cross section being given by:

$$\frac{d\sigma_{dA}}{d^2\mathbf{b}} = \sigma_{dp}(x, \mathbf{r}^2)\,T_A(\mathbf{b}) \ . \tag{5}$$

The associated predictions will be denoted by b - Non Sat hereafter. Moreover, the nuclear profile $T_A(\mathbf{b})$ will be described taking into account of all possible states of nucleon configurations in the nuclear wave function. We will assume that each nucleon in the nucleus has a Gaussian profile of width B_G centered at random positions sampled from a Woods-Saxon nuclear profile as follows [7]

$$T_A(\mathbf{b}) = \frac{1}{2\pi B_G} \sum_{i=1}^{A} \exp\left[-\frac{(\mathbf{b} - \mathbf{b}_i)^2}{2B_G}\right] \ . \tag{6}$$

The numerical calculations will be performed using the Sar*t*re event generator detailed in Ref. [8].

3. Results

In what follows we will analyze the photoproduction ($Q^2 \approx 0$) and electroproduction ($Q^2 \geq 1$ GeV^2) of vector mesons in electron - ion collisions, presenting predictions for the transverse

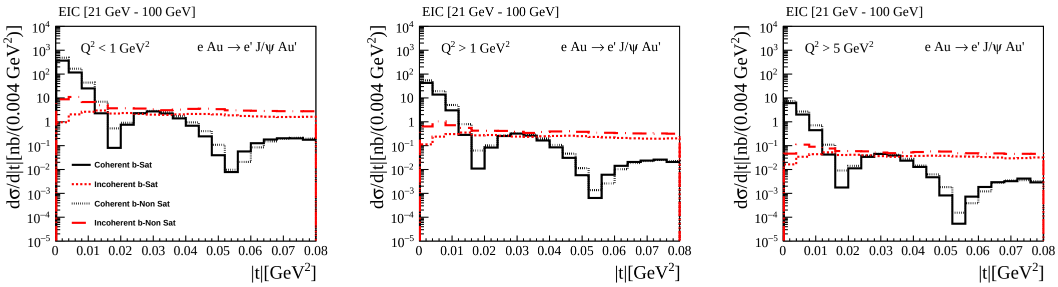

Figure 2: Transverse momentum distributions for the coherent and incoherent J/Ψ photoproduction in eAu collisions for the EIC energy, and different ranges of the photon virtuality Q^2.

momentum distributions. In Ref.[3] we have considered three different configurations for the electron and heavy ion energies, which correspond to those planned for the EIC, LHeC and FCC - eh. In this contribution, we will restrict our analysis to the EIC case and $A = 197$. Moreover, we will focus on the predictions for the squared momentum transfer (t) distribution , which is considered an important alternative to probe the QCD dynamics at high energies and provide information about the spatial distribution of the gluons in the target and about fluctuations of the color fields [9–11].

Our predictions for the squared momentum transfer (t) distribution are presented in Figs. 2 and 3 for the J/ψ and ϕ production, respectively. We present predictions for distinct ranges of the photon virtuality. One has that the coherent production dominates at small - $|t|$ and the incoherent ones at large values of the momentum transfer, in agreement with previous results [7, 10]. Such behaviours are expected, since the probability that the nucleus breaks up becomes larger when the momentum kick given to the nucleus is increased and becomes zero for $|t| \to 0$, where excited states cannot be produced. Moreover, one has that the coherent cross sections clearly exhibit the typical diffractive pattern, being characterized by a sharp forward diffraction peak, while the incoherent one is characterized by a flat t - dependence. We can see that the saturation effects reduce the normalization of the incoherent predictions, with the difference between the b-Sat and b-Non Sat predictions increasing with the energy and being larger for the ϕ production. Moreover, such difference also decreases at larger Q^2. For the coherent case, one also has that the normalization is suppressed by the saturation effects, with the impact being larger for the ϕ production. However, such suppression is smaller in comparison to that predicted for the incoherent production. As already observed in Refs. [10, 11], the position of the dips in the coherent predictions is sensitive to the presence of the saturation effects. Our results for the J/ψ production presented in Fig. 2, indicate that the position of the second dip is more dependent on description of the QCD dynamics, with the predictions becoming more distinct at larger energies. However, the difference between the b-Sat and b-NonSat predictions is small for this final state, which implies that the coherent J/ψ production is not ideal to discriminate between these two scenarios. In contrast, our results for the ϕ production, presented in Fig. 3, demonstrate that this final state is very sensitive to the saturation effects, with the position of the dips being strongly dependent on the model used to describe the dipole-nucleus cross section. One also has that the difference between the predictions decreases for larger photon virtualities. Our results for the ϕ production indicate that a future experimental analysis of this final state will be able to constrain the presence of the saturation effects, as well as

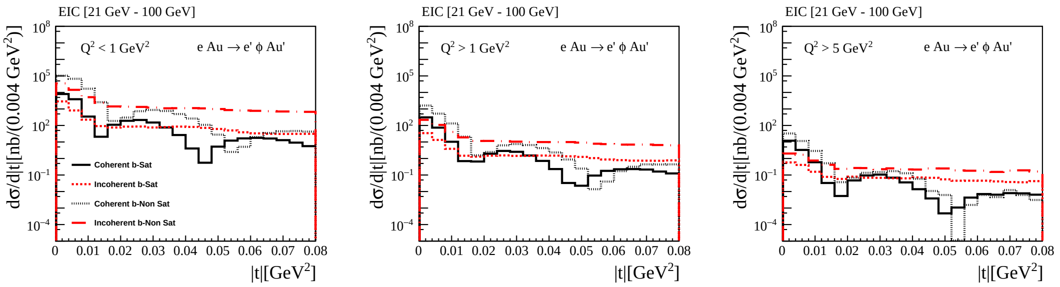

Figure 3: Transverse momentum distributions for the coherent and incoherent ϕ photoproduction in eAu collisions for the EIC energy and different ranges of the photon virtuality Q^2.

to probe the transition between the linear and non-linear regimes of the QCD dynamics.

Acknowledgments

This work was partially financed by the Brazilian funding agencies CNPq, CAPES, FAPERGS and INCT-FNA (process number 464898/2014-5).

References

[1] F. Gelis, E. Iancu, J. Jalilian-Marian and R. Venugopalan, Ann. Rev. Nucl. Part. Sci. **60**, 463 (2010); H. Weigert, Prog. Part. Nucl. Phys. **55**, 461 (2005); J. Jalilian-Marian and Y. V. Kovchegov, Prog. Part. Nucl. Phys. **56**, 104 (2006).

[2] A. Deshpande, R. Milner, R. Venugopalan and W. Vogelsang, Ann. Rev. Nucl. Part. Sci. **55**, 165 (2005).

[3] V. P. Gonçalves, D. E. Martins and C. R. Sena, Eur. Phys. J. A **57**, no.3, 82 (2021)

[4] H. Kowalski, L. Motyka and G. Watt, Phys. Rev. D **74**, 074016 (2006)

[5] V. P. Goncalves, M. V. T. Machado, B. D. Moreira, F. S. Navarra and G. S. dos Santos, Phys. Rev. D **96**, no. 9, 094027 (2017)

[6] R. J. Glauber, in Lecture in Theoretical Physics, Vol. 1, edited by W. E. Brittin, L. G. Duham (Interscience, New York, 1959); V. N. Gribov, Sov. Phys. JETP **29**, 483 (1969); Sov. Phys. JETP **30**, 709 (1970); A. H. Mueller, Nucl. Phys. B **335**, 115 (1990).

[7] M. Krelina, V. P. Goncalves and J. Cepila, Nucl. Phys. A **989**, 187-200 (2019)

[8] T. Toll and T. Ullrich, Comput. Phys. Commun. **185**, 1835-1853 (2014)

[9] N. Armesto and A. H. Rezaeian, Phys. Rev. D **90**, no. 5, 054003 (2014)

[10] V. P. Goncalves, F. S. Navarra and D. Spiering, Phys. Lett. B **768**, 299 (2017)

[11] V. P. Goncalves, F. S. Navarra and D. Spiering, Phys. Lett. B **791**, 299-304 (2019)